

UC Berkeley

UC Berkeley Previously Published Works

Title

Detection of the Order-to-Disorder Transition in Block Copolymer Electrolytes Using
Quadrupolar ^7Li NMR Splitting

Permalink

<https://escholarship.org/uc/item/6fs2f0vr>

Journal

ACS Macro Letters, 8(2)

ISSN

2161-1653

Authors

Grundy, Lorena S
Sethi, Gurmukh K
Galluzzo, Michael D
et al.

Publication Date

2019-02-19

DOI

10.1021/acsmacrolett.8b00809

Peer reviewed

Detection of the Order-to-Disorder Transition in Block Copolymer Electrolytes Using Quadrupolar ^7Li NMR Splitting

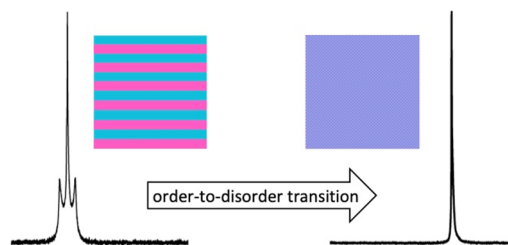
Lorena S. Grundy,[†] Gurmukh K. Sethi,^{‡,§} Michael D. Galluzzo,^{†,§} Whitney S. Loo,[†] Jacqueline A. Maslyn,^{†,§} Alexander A. Teran,[†] Jacob L. Thelen,[†] Ksenia Timachova,^{†,§} Jeffrey A. Reimer,^{†,§} Louis A. Madsen,[⊥] and Nitash P. Balsara^{*,†,§,||}

[†]Department of Chemical and Biomolecular Engineering and [‡]Department of Materials Science and Engineering, University of California, Berkeley, California 94720, United States

[§]Materials Science Division and ^{||}Joint Center for Energy Storage Research (JCESR), Lawrence Berkeley National Laboratory, Berkeley, California 94720, United States

[⊥]Department of Chemistry, Virginia Polytechnic Institute and State University, Blacksburg, Virginia 24061, United States

ABSTRACT: The order-to-disorder transition temperature (T_{ODT}) in a series of mixtures of polystyrene-*b*-poly(ethylene oxide) (SEO) and lithium bis(trifluoromethanesulfonyl)imide (LiTFSI) salt is identified by the disappearance of a quadrupolar ^7Li NMR triplet peak splitting above a critical temperature, where a singlet is observed. The macroscopic alignment of ordered domains required to produce a quadrupolar splitting occurs due to exposure to the NMR magnetic field. Alignment is confirmed using small-angle X-ray scattering (SAXS). The T_{ODT} determined by NMR is consistent with that determined using SAXS.



Block copolymers (with or without salt added) self-assemble into a variety of ordered phases.^{1,2} At sufficiently high temperatures, entropy dominates, resulting in the formation of a disordered phase. Established experimental approaches for locating the order-to-disorder transition temperature (T_{ODT}) include small-angle X-ray scattering (SAXS),^{3,4} small-angle neutron scattering (SANS),⁵ birefringence,⁶ and rheology.^{7–10} There is increasing interest in the properties of mixtures of block copolymers and fluorine-containing lithium salts due to their relevance in lithium batteries. Locating the T_{ODT} in these systems is important, as microscopic morphology has a profound impact on bulk properties such as mechanical rigidity and ionic conductivity.^{11,12}

While nuclear magnetic resonance spectroscopy (NMR) is often used to study the chemical environment of lithiated compounds, it is rarely used to study block copolymer electrolyte systems. Both naturally occurring lithium isotopes, ^6Li and ^7Li , can be observed using NMR, but ^7Li is chosen most commonly due to its higher natural abundance and NMR sensitivity.¹³ Several researchers have used NMR to study these polymer electrolytes.^{13–17} In these studies, the NMR peak corresponding to lithium appears as a single line. While lithium spin–spin (scalar J or dipole–dipole D) coupling to other NMR-active nuclei such as protons (^1H) or fluorine (^{19}F) is possible,^{18,19} to our knowledge, lithium splitting due to such coupling has never been observed in polymeric systems. Previous studies of lithium cations in polymer electrolytes report only ^7Li line broadening due to heteronuclear dipolar interactions.²⁰

The quadrupolar moment of the spin-3/2 ^7Li nucleus enables splitting of the NMR signal into a triplet when the lithium atoms experience a nonzero average electric field gradient (EFG).²¹ (^{19}F , however, is spin-1/2 and therefore cannot exhibit quadrupolar splitting.) A triplet peak splitting will occur only when lithium cations are sampling an EFG environment with an overall degree of alignment, as in a macroscopically aligned sample. It is therefore not surprising that in the vast majority of experiments ^7Li spectra appear as single peaks. However, recent work has demonstrated that strong magnetic fields can uniformly align the domains of block copolymers, allowing for a higher degree of average orientation.²² Earlier work has shown that quadrupolar splitting can be used to investigate magnetic-field-aligned biological membrane bicelles²³ and alignment in polymers using labeled probe molecules,²⁴ including D_2O -swollen block copolymers aligned by a casting process,²⁵ but never with lithium ions in block copolymers. In previous work on aligned polymer electrolytes with magnetic fillers, quadrupolar interactions have been shown only to cause line broadening, due to a broad distribution in domain orientation.¹⁵

Herein, we report the presence of quadrupolar ^7Li triplet spectra in lamellae-forming mixtures of block copolymers and a lithium salt oriented through exposure to the NMR magnetic field. The splittings disappear when the sample is disordered,

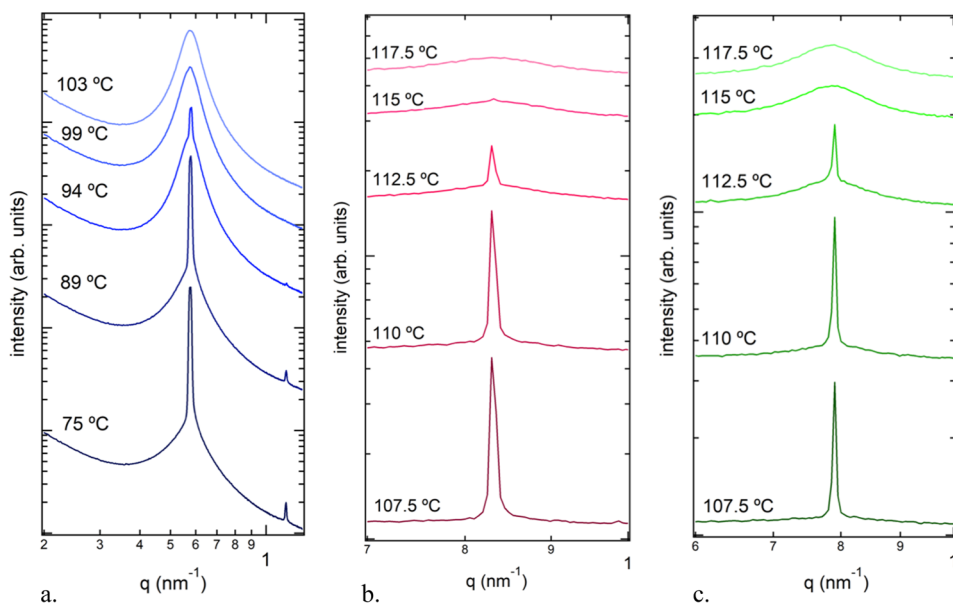


Figure 1. SAXS profiles at a range of temperatures for SEO(3.3–2.6) $r = 0.02$ (a), SEO(1.7–1.4) $r = 0.075$ (b), and SEO(1.5–2.0) $r = 0.125$ (c).

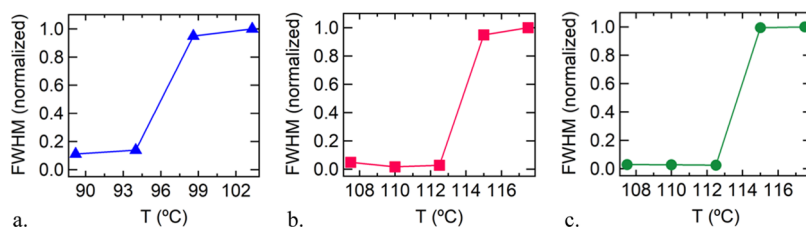


Figure 2. Plots of the full-width at half-maximum (FWHM) of the primary scattering peak at a range of temperatures for SEO(3.3–2.6) $r = 0.02$ (a), SEO(1.7–1.4) $r = 0.075$ (b), and SEO(1.5–2.0) $r = 0.125$ (c).

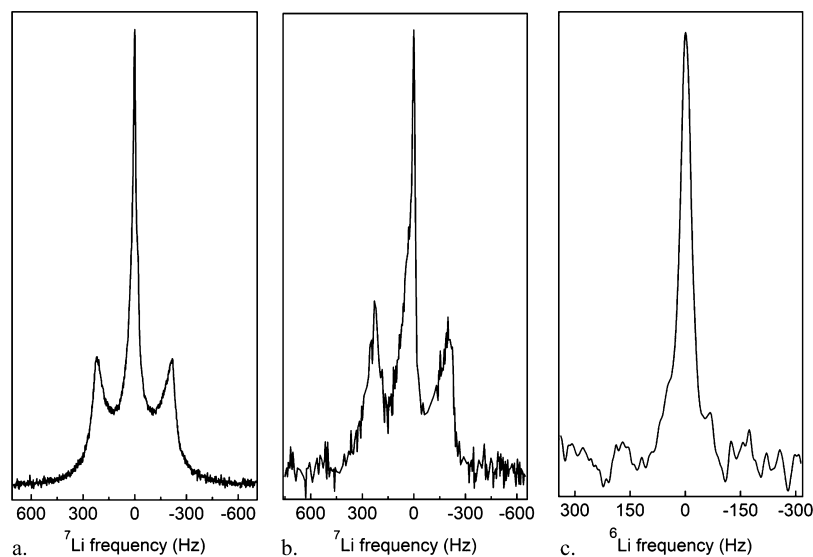


Figure 3. NMR spectra of SEO(1.7–1.4) $r = 0.075$ at 90 °C for ${}^7\text{Li}$ (a), ${}^{19}\text{F}$ -decoupled ${}^7\text{Li}$ (b), and ${}^6\text{Li}$ (c).

indicating that NMR can be used to detect the order-to-disorder transition.

SAXS profiles of three electrolytes at selected temperatures are shown in Figure 1. The scattering from these samples was isotropic, as is typically the case for block copolymers in the absence of external fields. In Figure 1a, we show SAXS profiles of polystyrene-*b*-poly(ethylene oxide) (SEO) with a molecular

weight of 3.3 kg mol⁻¹ of polystyrene (PS) and 2.6 kg mol⁻¹ of poly(ethylene oxide) (PEO) mixed with a lithium bis-(trifluoromethanesulfonyl)imide (LiTFSI) salt at a concentration of 0.02 lithium ions per ethylene oxide (EO) moiety (SEO(3.3–2.6) $r = 0.02$). At 75 and 89 °C, we see two scattering peaks, a sharp primary scattering peak at $q = q^* = 0.60 \text{ nm}^{-1}$ and a higher-order scattering peak at $q = 2q^*$. This

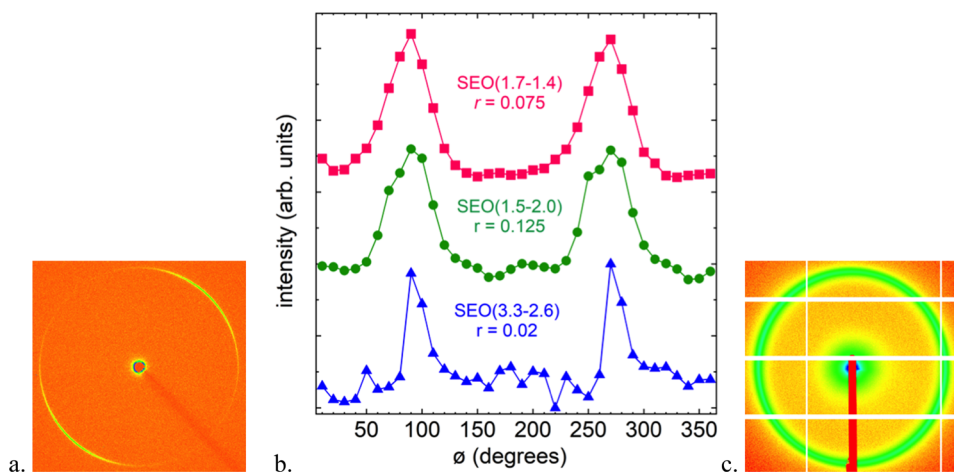


Figure 4. Two-dimensional SAXS profile of magnetic-field-aligned SEO(1.7–1.4) $r = 0.075$ (a), plots of normalized scattering intensity as a function of angle, $I(\phi)$, for aligned SEO(1.7–1.4) $r = 0.075$ (red ■), SEO(1.5–2.0) $r = 0.125$ (green ●), and SEO(3.3–2.6) $r = 0.02$ (blue ▲) (b), and the two-dimensional SAXS profile of SEO(1.7–1.4) $r = 0.075$ not exposed to the magnetic field (c).

indicates the presence of a lamellar phase in this temperature range. At 99 and 103 °C, we observe a single broad scattering peak due to disordered concentration fluctuations.^{1,26} The scattering profile at 94 °C is a superposition of a broad peak and a narrow peak, indicating coexistence of ordered and disordered phases. This coexistence is required by the Gibbs phase rule.^{27,28} Qualitatively similar results are observed for the other two electrolytes, SEO(1.7–1.4) $r = 0.075$ (Figure 1b) and SEO(1.5–2.0) $r = 0.125$ (Figure 1c). Based on previous studies,²⁹ we can assert that the ordered phases are lamellar. (The higher-order peaks are outside the q window of some of our experiments.) In these experiments, we also observe coexistence of ordered and disordered phases. In Figure 2, we plot the full-width at half-maximum (FWHM) of the primary scattering peak as a function of temperature. In cases where broad and sharp peaks coexist, we fit two curves and report the FWHM of the sharp peak. The temperature change that results in complete disordering of the partially ordered sample is used to define the T_{ODT} . For SEO(3.3–2.6) $r = 0.02$, $T_{\text{ODT}} = 96.5 \pm 3$ °C; for SEO(1.7–1.4) $r = 0.075$, $T_{\text{ODT}} = 114 \pm 2$ °C; and for SEO(1.5–2.0) $r = 0.125$, $T_{\text{ODT}} = 114 \pm 2$ °C.

The ^7Li NMR spectrum of SEO(1.7–1.4) $r = 0.075$ taken at 90 °C on a 14.1 T instrument is shown in Figure 3a. The spectrum contains a primary peak and two satellites spaced 1.8 ppm (420 Hz) apart. In principle, this splitting could be due to indirect spin–spin coupling of lithium to fluorine (^{19}F ; $I = 1/2$), the only significantly naturally abundant NMR-observable nucleus in the anion. We therefore performed ^{19}F -decoupled ^7Li NMR,³⁰ and the resulting spectrum is shown in Figure 3b. The persistence of a triplet in this spectrum indicates that the splitting seen in Figure 3a is not due to spin–spin coupling of lithium to fluorine.

Quadrupolar splitting is the most likely explanation for the presence of a triplet in the ^7Li NMR spectrum, as ^7Li is a spin $I = 3/2$ nucleus with a moderate quadrupole moment (–40.1 mbarn).³¹ We tested this hypothesis by measuring the ^6Li spectrum of SEO(1.7–1.4) $r = 0.075$, as ^6Li is a spin $I = 1$ nucleus with a very weak quadrupole moment (–0.808 mbarn). If heteronuclear coupling was responsible for the splitting, the ^6Li spectrum would also show a triplet with a spacing of 1.8 ppm (160 Hz), while if residual quadrupolar splitting was the cause, such a triplet would not appear in the

^6Li spectrum. The result of this experiment is shown in Figure 3c, where only a single peak is observed. In principle, the spin $I = 1$ ^6Li nucleus should exhibit doublet quadrupolar splitting, but the low quadrupolar moment of ^6Li causes the predicted splitting to be 26 Hz (0.36 ppm) in this case,²¹ which is smaller than the spectral resolution of the measurement. Additional confirmation of our conclusion based on the ^{19}F -decoupled ^7Li and the ^6Li NMR spectra can be found in the peak integrals of the ^7Li spectrum: triplets caused by spin–spin coupling have a peak ratio of 1:2:1, while those caused by quadrupolar splitting have a ratio of 3:4:3.³² When the peaks in Figure 3a are fit to Lorentzian curves and integrated, they have a ratio of 3.0:4.0:3.3, further indicating that the origin of the triplet peak pattern is quadrupolar.

Our observation of quadrupolar splitting indicates interactions between the ^7Li nuclei and local EFGs which could, in principle, be generated by an ordered phase composed of alternating PS-rich and PEO-rich lamellae. However, if these lamellae were randomly oriented with respect to the applied magnetic field direction, the effect of the concomitant randomly oriented electric fields would cancel, precluding quadrupolar splitting. Therefore, the splitting in SEO(1.7–1.4) $r = 0.075$ could arise only if the lamellae were not randomly oriented.

Recent work by Osuji and co-workers has shown that block copolymer domains can align spontaneously under an applied magnetic field, even if the chains are devoid of mesogenic units.²² In order to test whether this is the case in SEO(1.7–1.4) $r = 0.075$, a SAXS sample of the electrolyte was placed in an NMR tube, heated above the T_{ODT} outside the magnet to erase thermal history and prior alignment, and then inserted into the 14.1 T NMR magnet, where it was cooled to 90 °C (a temperature that is below the T_{ODT}). After 5 min, it was rapidly removed from the NMR magnet and quenched in liquid nitrogen to lock in the morphology that was relevant for our NMR experiment. (Crystallization of the PEO-rich lamellae can distort the morphology of block copolymers.^{33,34} The quench vitrifies the PEO, preventing crystallization.) The sample was then studied using SAXS, yielding the two-dimensional pattern shown in Figure 4a. The presence of anisotropic arcs in the SAXS pattern indicates alignment of the lamellae. The experiment was repeated for the other two

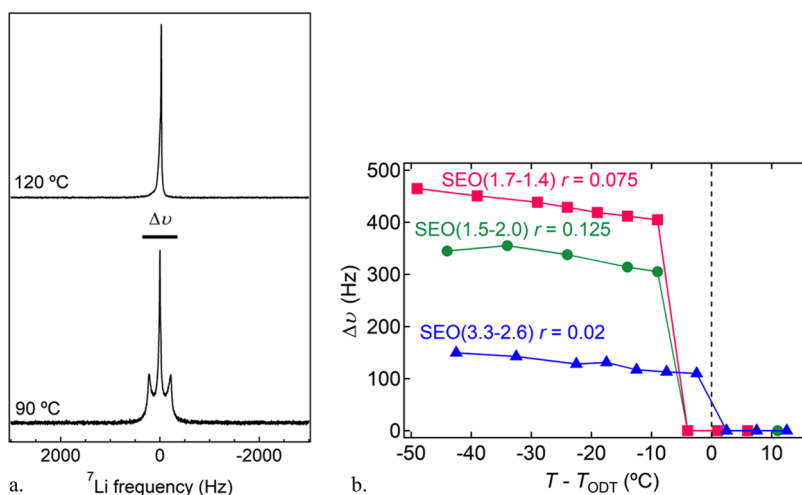


Figure 5. NMR spectra of SEO(1.7–1.4) $r = 0.075$ at 90 and 120 $^\circ\text{C}$ (a) and the distance between the two satellite peaks, $\Delta\nu$, in ^7Li NMR quadrupolar triplets versus temperature, normalized by subtracting the SAXS T_{ODT} , for SEO(1.7–1.4) $r = 0.075$ (red \blacksquare), SEO(1.5–2.0) $r = 0.125$ (green \bullet), and SEO(3.3–2.6) $r = 0.02$ (blue \blacktriangle) (b).

electrolytes, and the results are qualitatively similar. These results are shown in the form of normalized scattering intensity in the vicinity of the primary peak, I , versus the azimuthal angle, ϕ , in Figure 4b. (Our experimental setup does not enable determination of the relationship between the magnetic field direction and ϕ .) A control sample of SEO(1.7–1.4) $r = 0.075$ was exposed to the same conditions but was never placed in the magnet. The SAXS pattern of this sample is more-or-less isotropic (Figure 4c), indicating that alignment in the other samples is a result of magnetic field exposure.

The attribution of ^7Li NMR triplets to quadrupolar interactions caused by aligned lamellae requires this behavior to disappear in disordered samples. In Figure 5a, we show the NMR spectra of SEO(1.7–1.4) $r = 0.075$ obtained at 90 and 120 $^\circ\text{C}$. We define $\Delta\nu$ as the difference between the locations of the satellite triplet peaks. When there is no splitting, as is the case at 120 $^\circ\text{C}$, $\Delta\nu$ is zero. Figure 5b presents $\Delta\nu$ as a function of temperature for all three electrolytes. In these measurements, samples were first annealed outside the magnet to remove any previous alignment, then inserted into the magnet, where measurements were taken upon cooling after 10 min of equilibration at each temperature. In all cases, the first temperature studied was above T_{ODT} (as determined by SAXS). The triplet splittings appear below the T_{ODT} , confirming our assignment of the triplet splitting to quadrupolar interactions caused by an aligned ordered morphology which arises due to exposure to the NMR magnetic field. There is a 5 $^\circ\text{C}$ difference between the NMR and SAXS signatures of T_{ODT} in SEO(1.7–1.4) $r = 0.075$ and SEO(1.5–2.0) $r = 0.125$. Given the large differences in sample geometry and instrumentation, we attribute this shift to imprecise temperature calibrations and complications arising from the presence of coexistence windows in the vicinity of the T_{ODT} .^{27,28}

The data in Figure 5b show that, for a given electrolyte, $\Delta\nu$ is a weak function of temperature below the T_{ODT} . The splitting magnitude in the ordered phase likely depends on a variety of parameters, such as salt concentration, degree of alignment, ion dynamics, domain spacing, anisotropic chain stretching, and the nature of the interface between PS-rich and PEO-rich lamellae.^{24,25,35} While further work is needed to elucidate the relationship between $\Delta\nu$ and the ordered

morphology, we have established that the disappearance of NMR quadrupolar splitting is a definitive signature of the order-to-disorder transition in magnetic-field-oriented lamellae-forming block copolymer electrolytes.

In summary, we have demonstrated that ^7Li NMR can be used to locate the T_{ODT} in block copolymer electrolytes. The electrolytes tested here have lamellar morphology in the ordered state, which is oriented through exposure to the strong magnetic field present in an NMR instrument. The orientation of lamellae is confirmed using SAXS. The anisotropic material environment causes NMR spectra of the quadrupolar ^7Li nucleus to display a triplet splitting. The triplet becomes a singlet above the T_{ODT} due to the disappearance of the anisotropic environment. The T_{ODT} determined by NMR agrees well with that determined by SAXS experiments.

EXPERIMENTAL SECTION

Polymer Synthesis and Characterization. The polystyrene-*b*-poly(ethylene oxide) (SEO) block copolymers in this study were synthesized, purified, and characterized using methods described by Teran et al.²⁹ and Hadjichristidis et al.³⁶ The polymers are denoted SEO($M_{\text{PS}}-M_{\text{PEO}}$), where M_{PS} and M_{PEO} are the number-averaged molecular weights of PS and PEO, respectively, in kg mol^{-1} .

Preparation of Electrolytes. The salt-containing copolymers were prepared using methods described by Thelen et al.²⁸ Argon gloveboxes from Vacuum Atmospheres Company were used for all sample preparation. The molar ratio of lithium ions to ethylene oxide (EO) units, r , is used to quantify salt concentration. Table 1 describes the electrolytes used in this study.

Table 1. Characteristics of Electrolytes Used in This Study

polymer	M_{PS} (kg mol^{-1})	M_{PEO} (kg mol^{-1})	r
SEO(1.7–1.4)	1.7	1.4	0.075
SEO(1.5–2.0)	1.5	2.0	0.125
SEO(3.3–2.6)	3.3	2.6	0.020

SAXS Measurements. SAXS samples, consisting of electrolyte in a rubber spacer sandwiched between two Kapton windows, were prepared according to methods described by Loo et al.³⁷ Experiments were conducted at the Advanced Light Source beamline 7.3.3 at Lawrence Berkeley National Lab³⁸ and beamline 1–5 at the Stanford Synchrotron Radiation Lightsources (SSRL) at SLAC National Accelerator Laboratory. Measurements were taken upon cooling

from 130 °C in steps of 2.5 to 60 °C, after 20 min annealing at each temperature.

NMR Spectroscopy. NMR measurements were performed at 14.1 T using a 600 MHz Bruker Avance III spectrometer with a 5 mm PABBO direct detection broad-band probe (BB-1H/D Z-GRD) and a variable-temperature unit. Measurements were performed on ⁷Li at a resonance frequency of 233.23 MHz with a 90° pulse time of 13.5 μs at a power level of -2 dB, acquisition time of 0.4 s, and relaxation delay of 1 s and on ⁶Li at a resonance frequency of 88.32 MHz with a 90° pulse time of 16.75 μs at a power level of -2 dB, acquisition time of 0.58 s, and relaxation delay of 1 s. Additionally, ⁷Li measurements were acquired with ¹⁹F decoupling using an inverse-gated decoupling sequence³⁰ on resonance with δ(¹⁹F) frequencies at -78 ppm at 1.66 W. The acquisition time was 0.114 s and the relaxation delay 1.5 s. Before each experiment, prior to exposure to the magnetic field, samples were heated above *T*_{ODT} and allowed to cool to remove previous alignment. When temperature was varied during NMR experiments, samples were allowed to equilibrate for 10 min at each new temperature, and the first temperature studied was above the *T*_{ODT} determined by SAXS.

SAXS Measurements of Magnetically Aligned Samples.

SAXS samples were prepared as described above and inserted into 5 mm NMR tubes in an argon glovebox. Because the polymer was protected by Kapton windows, it did not experience shear stress upon insertion into the tubes. The samples were heated above *T*_{ODT} and annealed at 90 °C for 5 min in the same 14.1 T instrument used for NMR experiments, while control samples were exposed to the same conditions without the presence of a magnetic field. All samples were quenched at -196 °C for 5 min to prevent morphological changes upon crystallization. They were then removed from NMR tubes in an argon glovebox and analyzed with SAXS at room temperature using the methods described above. Two-dimensional scattering profiles were divided into sectors which were integrated in the vicinity of the primary scattering peak to determine the azimuthal dependence of the scattered intensity, *I*(φ).

AUTHOR INFORMATION

Corresponding Author

*E-mail: nbalsara@berkeley.edu.

ORCID

Lorena S. Grundy: 0000-0001-7706-2216

Gurmukh K. Sethi: 0000-0002-8966-385X

Whitney S. Loo: 0000-0002-9773-3571

Jacqueline A. Maslyn: 0000-0002-6481-2070

Jacob L. Thelen: 0000-0003-0026-4404

Ksenia Timachova: 0000-0001-8200-3552

Jeffrey A. Reimer: 0000-0002-4191-3725

Louis A. Madsen: 0000-0003-4588-5183

Nitash P. Balsara: 0000-0002-0106-5565

Notes

The authors declare no competing financial interest.

ACKNOWLEDGMENTS

Primary funding for this work was provided by the National Science Foundation through Award DMR-1505444. Work at the Advanced Light Source, which is a DOE Office of Science User Facility, was supported by contract no. DE-AC02-05CH11231. Work at the Stanford Synchrotron Radiation Light Source, a user facility at SLAC National Accelerator Laboratory, was supported by the U.S. Department of Energy, Office of Science, Office of Basic Energy Sciences under contract no. DE-AC02-76SF00515. The work of L.A.M. was also supported in part by the National Science Foundation under Award DMR-1810194. We are grateful to the UC Berkeley College of Chemistry NMR Facility, and especially

Hasan Celik and Nanette Jarenwattananon, for their productive conversations and help with instrumentation and to David Halat for helpful discussions.

REFERENCES

- (1) Leibler, L. Theory of Microphase Separation in Block Copolymers. *Macromolecules* **1980**, *13* (6), 1602–1617.
- (2) Bates, F. S.; Fredrickson, G. H. Block Copolymer Thermodynamics: Theory and Experiment. *Annu. Rev. Phys. Chem.* **1990**, *41* (1), 525–557.
- (3) Gervais, M.; Gallot, B. Phase Diagram and Structural Study of Polystyrene–Poly(ethylene oxide) Block Copolymers, 1. *Makromol. Chem.* **1973**, *171*, 157–178.
- (4) Sakamoto, N.; Hashimoto, T. Order-Disorder Transition of Low Molecular Weight Polystyrene-*block*-Polyisoprene. I. SAXS Analysis of Two Characteristic Temperatures. *Macromolecules* **1995**, *28* (20), 6825–6834.
- (5) Bates, F. S.; Rosedale, J. H.; Fredrickson, G. H. Fluctuation Effects in a Symmetric Diblock Copolymer Near the Order-Disorder Transition. *J. Chem. Phys.* **1990**, *92* (10), 6255–6270.
- (6) Balsara, N. P.; Perahia, D.; Safinya, C. R.; Tirrell, M.; Lodge, T. P. Birefringence Detection of the Order-to-Disorder Transition in Block Copolymer Liquids. *Macromolecules* **1992**, *25* (15), 3896–3901.
- (7) Chung, C. I.; Gale, J. C. Newtonian Behavior of a Styrene-Butadiene-Styrene Block Copolymer. *J. Polym. Sci., Polym. Phys. Ed.* **1976**, *14*, 1149–1156.
- (8) Han, C. D.; Kim, J.; Kim, J. K. Determination of the Order-Disorder Transition Temperature of Block Copolymers. *Macromolecules* **1989**, *22* (1), 383–394.
- (9) Adams, J. L.; Graessley, W. W.; Register, R. A. Rheology and the Microphase Separation Transition in Styrene-Isoprene Block Copolymers. *Macromolecules* **1994**, *27* (21), 6026–6032.
- (10) Rosedale, J. H.; Bates, F. S. Rheology of Ordered and Disordered Symmetric Poly(ethylenepropylene)-poly(ethylene) Diblock Copolymers. *Macromolecules* **1990**, *23* (8), 2329–2338.
- (11) Singh, M.; Odusanya, O.; Wilmes, G. M.; Eitouni, H. B.; Gomez, E. D.; Patel, A. J.; Chen, V. L.; Park, M. J.; Fragouli, P.; Iatrou, H.; Hadjichristidis, N.; Cookson, D.; Balsara, N. P. Effect of Molecular Weight on Mechanical and Electrical Properties of Block Copolymer Electrolytes. *Macromolecules* **2007**, *40* (13), 4578–4585.
- (12) Teran, A. A.; Mullin, S. A.; Hallinan, D. T., Jr.; Balsara, N. P. Discontinuous Changes in Ionic Conductivity of a Block Copolymer Electrolyte through an Order-Disorder Transition. *ACS Macro Lett.* **2012**, *1*, 305–309.
- (13) Abbrent, S.; Greenbaum, S. Recent Progress in NMR Spectroscopy of Polymer Electrolytes for Lithium Batteries. *Curr. Opin. Colloid Interface Sci.* **2013**, *18*, 228–244.
- (14) Dai, Y.; Wang, Y.; Greenbaum, S. G.; Bajue, S. A.; Golodnitsky, D.; Ardel, G.; Strauss, E.; Peled, E. Electrical, Thermal, and NMR Investigation of Composite Solid Electrolytes Based on PEO, LiI and High Surface Area Inorganic Oxides. *Electrochim. Acta* **1998**, *43* (10–11), 1557–1561.
- (15) Golodnitsky, D.; Livshits, E.; Kovarsky, R.; Peled, E.; Chung, S. H.; Suarez, S.; Greenbaum, S. G. New Generation of Ordered Polymer Electrolytes for Lithium Batteries. *Electrochim. Solid-State Lett.* **2004**, *7* (11), A412–A415.
- (16) Trease, N. M.; Köster, T. K.-J.; Grey, C. P. *In Situ* NMR Studies of Lithium Ion Batteries. *Electrochim. Soc. Interface* **2011**, *20* (3), 69–73.
- (17) Timachova, K.; Villaluenga, I.; Cirrincione, L.; Gobet, M.; Bhattacharya, R.; Jiang, X.; Newman, J.; Madsen, L. A.; Greenbaum, S. G.; Balsara, N. P. Anisotropic Ion Diffusion and Electrochemically Driven Transport in Nanostructured Block Copolymer Electrolytes. *J. Phys. Chem. B* **2018**, *122* (4), 1537–1544.
- (18) Günther, H. Selected Topics from Recent NMR Studies of Organolithium Compounds. *J. Braz. Chem. Soc.* **1999**, *10* (4), 241–262.

- (19) Fernández, I.; Oña-Burgos, P.; Armbruster, F.; Krummenacher, I.; Breher, F. ${}^7\text{Li}$, ${}^{15}\text{N}$ Heteronuclear Multiple Quantum Shift Correlation—a Fast and Reliable 2D NMR Method on Natural Abundant Nuclei. *Chem. Commun.* **2009**, *18*, 2586–2588.
- (20) Pawlicka, A.; Donoso, J. P.; Abbrent, S.; Greenbaum, S. In *Polymer Electrolytes: Fundamentals and Applications*; Sequeria, C., Santos, D., Eds.; Woodhead: Cambridge, 2010; pp 112–118 and 278–313.
- (21) Levitt, M. H. *Spin Dynamics: Basics of Nuclear Magnetic Resonance*, 2nd ed.; Wiley: New York, 2008; p 209.
- (22) Rokhlenko, Y.; Gopinadhan, M.; Osuji, C. O.; Zhang, K.; O'Hern, C. S.; Larson, S. R.; Gopalan, P.; Majewski, P. W.; Yager, K. G. Magnetic Alignment of Block Copolymer Microdomains by Intrinsic Chain Anisotropy. *Phys. Rev. Lett.* **2015**, *115*, 258302.
- (23) Prosser, R. S.; Evanics, F.; Kitevski, J. L.; Al-Abdul-Wahid, M. S. Current Applications of Bicelles in NMR Studies of Membrane-Associated Amphiphiles and Proteins. *Biochemistry* **2006**, *45* (28), 8453–8465.
- (24) Deloche, B.; Samulski, E. T. Short-Range Nematic-like Orientational Order in Strained Elastomers: A Deuterium Magnetic Resonance Study. *Macromolecules* **1981**, *14* (3), 575–581.
- (25) Hou, J.; Li, J.; Madsen, J. A. Anisotropy and Transport in Poly(arylene ether sulfone) Hydrophilic-Hydrophobic Block Copolymers. *Macromolecules* **2010**, *43* (1), 347–353.
- (26) Bates, F. S.; Rosedale, J. H.; Fredrickson, G. H.; Glinka, C. J. Fluctuation-Induced First-Order Transition of an Isotropic System to a Periodic State. *Phys. Rev. Lett.* **1988**, *61* (19), 2229–2232.
- (27) Nakamura, I.; Balsara, N. P.; Wang, Z. G. First-Order Disordered-to-Lamellar Phase Transition in Lithium Salt-Doped Block Copolymers. *ACS Macro Lett.* **2013**, *2* (6), 478–481.
- (28) Thelen, J. L.; Teran, A. A.; Wang, X.; Garetz, B. A.; Nakamura, I.; Wang, Z. G.; Balsara, N. P. Phase Behavior of a Block Copolymer/Salt Mixture through the Order-to-Disorder Transition. *Macromolecules* **2014**, *47* (8), 2666–2673.
- (29) Teran, A. A.; Balsara, N. P. Thermodynamics of Block Copolymers with and without Salt. *J. Phys. Chem. B* **2014**, *118*, 4–17.
- (30) Freeman, R.; Hill, H. D. W.; Kaptein, R. Proton-Decoupled NMR Spectra of Carbon-13 With the Nuclear Overhauser Effect Suppressed. *J. Magn. Reson.* **1972**, *7* (3), 327–329.
- (31) Pyykkö, P. Year-2017 Nuclear Quadrupole Moments. *Mol. Phys.* **2018**, *116* (10), 1328–1338.
- (32) Man, P. P.; Klinowski, J.; Trokner, A.; Zanni, H.; Papon, P. Selective and non-Selective NMR Excitation of Quadrupolar Nuclei in the Solid State. *Chem. Phys. Lett.* **1988**, *151*, 143–150.
- (33) Loo, Y.; Register, R. A.; Ryan, A. J. Modes of Crystallization in Block Copolymer Microdomains: Breakout, Templated, and Confined. *Macromolecules* **2002**, *35* (6), 2365–2374.
- (34) Ho, R. M.; Lin, F. H.; Tsai, C. C.; Lin, C. C.; Ko, B. T.; Hsiao, B. S.; Sics, I. Crystallization-Induced Undulated Morphology in Polystyrene-*b*-Poly(L-lactide) Block Copolymer. *Macromolecules* **2004**, *37* (16), 5985–5994.
- (35) Wang, Y.; Gao, J.; Dingemans, T. J.; Madsen, L. A. Molecular Alignment and Ion Transport in Rigid Rod Polyelectrolyte solutions. *Macromolecules* **2014**, *47* (9), 2984–2992.
- (36) Hadjichristidis, N.; Iatrou, H.; Pispas, S.; Pitsikalis, M. Anionic Polymerization: High Vacuum Techniques. *J. Polym. Sci., Part A: Polym. Chem.* **2000**, *38*, 3211–3234.
- (37) Loo, W. S.; Jiang, X.; Maslyn, J. A.; Oh, H. J.; Zhu, C.; Downing, K. H.; Balsara, N. P. Reentrant Phase Behavior and Coexistence in Asymmetric Block Copolymer Electrolytes. *Soft Matter* **2018**, *14*, 2789–2795.
- (38) Hexemer, A.; Bras, W.; Glossinger, J.; Schaible, E.; Gann, E.; Kirian, R.; MacDowell, A.; Church, M.; Rude, B.; Padmore, H. A SAXS/WAXS/GISAXS Beamline with Multilayer Monochromator. *J. Phys.: Conf. Ser.* **2010**, *247*, 1–11.